This is a repository copy of *Pulsed-Field Gradient NMR Self Diffusion and Ionic Conductivity Measurements for Liquid Electrolytes Containing LiBF₄ and Propylene Carbonate*.

Article:

Accepted Manuscript

Title: Pulsed-Field Gradient NMR Self Diffusion and Ionic Conductivity Measurements for Liquid Electrolytes Containing LiBF$_4$ and Propylene Carbonate

Author: P.M. Richardson A.M. Voice I.M. Ward

Please cite this article as: P.M. Richardson, A.M. Voice, I.M. Ward, Pulsed-Field Gradient NMR Self Diffusion and Ionic Conductivity Measurements for Liquid Electrolytes Containing LiBF$_4$ and Propylene Carbonate, *Electrochimica Acta* (2014), http://dx.doi.org/10.1016/j.electacta.2014.03.072

This is a PDF file of an unedited manuscript that has been accepted for publication. As a service to our customers we are providing this early version of the manuscript. The manuscript will undergo copyediting, typesetting, and review of the resulting proof before it is published in its final form. Please note that during the production process errors may be discovered which could affect the content, and all legal disclaimers that apply to the journal pertain.

Pulsed-Field Gradient NMR Self Diffusion and Ionic Conductivity Measurements for Liquid Electrolytes Containing LiBF$_4$ and Propylene Carbonate

P.M. Richardson*, A.M. Voice, I.M. Ward

Soft Matter Physics, School of Physics and Astronomy, University of Leeds, Leeds, LS2 9JT, UK

Abstract

Liquid electrolytes have been prepared using lithium tetrafluoroborate (LiBF$_4$) and propylene carbonate (PC). Pulsed-field gradient nuclear magnetic resonance (PFG-NMR) measurements were taken for the cation, anion and solvent molecules using lithium (^{7}Li), fluorine (^{19}F) and hydrogen (^{1}H) nuclei, respectively. It was found that lithium diffusion was slow compared to the much larger fluorinated BF$_4$ anion likely resulting from a large solvation shell of the lithium. Ionic conductivity and viscosity have also been measured for a range of salt concentrations and temperatures. By comparing the measured conductivity with a ideal predicted conductivity derived from the Nernst-Einstein equation and self diffusion coefficients the degree of ionic association of the anion and cation was determined and was observed to increase with salt concentration and temperature. Using the measured viscosity and self diffusion coefficients the effective radius of each of the species was determined for various salt concentrations.

Keywords: NMR, liquid electrolyte, conductivity, ionic association

1. Introduction

Liquid electrolytes are of scientific interest due to their use in electrochemical devices, they consist of an ionic salt dissolved in a solvent. The choices of these materials play a vital role in determining the dynamics of the ions in solution. Usually lithium based

*Corresponding Author

Email addresses: phypmr@leeds.ac.uk (P.M. Richardson), a.m.voice@leeds.ac.uk (A.M. Voice), i.m.ward@leeds.ac.uk (I.M. Ward)

salts are chosen due to the high charge density that the lithium ions possess. The anion is usually chosen to be relatively large in size to create an uneven charge distribution, which promotes ionic dissociation. Since the primary application of liquid electrolytes is in electrochemical devices it is important for the ions to be relatively mobile and free to conduct, therefore a low ionic association is desired in these systems. In this study lithium tetrafluoroborate (LiBF$_4$) was dissolved in propylene carbonate (PC) at molar concentrations between 0.1-1.5M (mol dm^{-3}), which corresponded to molal concentrations between 0.08-1.37 mol kg^{-1}. The aim of this current research is to probe the motion of the ions in solution as a function of both temperature and salt concentration. A secondary aim of this paper is to pave the way for future publications on polymer gel electrolytes; which involve adding polymer to a liquid electrolyte at high temperatures to form a porous polymer network filled with liquid electrolyte.

Following the pioneering research of Wright [1] and Armand [2] into solid polymer electrolytes and their potential for use in lithium batteries, thermo-reversible polymer gel electrolytes (PGEs)[3, 4] have been studied at the University of Leeds with the introduction of solvents [5, 6]. These gel electrolytes combine the high ionic mobility of conventional liquid electrolytes with the mechanical advantage of incorporating a polymer. Typical PGEs comprise of poly(vinylidene) fluoride (PVDF), propylene carbonate (PC) and lithium salts[7, 8]. A first stage in developing a fundamental understanding of these gel electrolytes has been to study the behaviour of model liquid electrolyte solutions. Understanding the transport properties of these liquid electrolytes is important to use as a basis of comparison. Therefore in this paper the pure liquid electrolyte system is reported which will aid in the understanding of future papers concerning polymer gel electrolytes.

The experimental techniques which have been used to understand the dynamics of the current system are pulsed-field gradient NMR, dielectric spectroscopy and viscosity measurements. NMR has been proven to be a valuable tool for understanding the dynamics of liquid solutions via different techniques. In a previous publication it has been shown that the use of NMR relaxation times yield valuable information about the rotational and translational motion of the ions in solution [9]. In this paper pulsed-field gradient NMR was used in order to measure the translational self diffusion constants.

2

It is possible to isolate individual nuclei using the corresponding resonant frequency. In this paper results for ^{1}H, ^{7}Li and ^{19}F nuclei have been measured which corresponds to the solvent molecules, lithium cation and fluorinated BF_4 anions, respectively. Therefore measuring the diffusion constant in this manner can yield information about the dynamics of each constituent within the liquid electrolytes; and these have been observed with changing temperature and salt concentration. Pulsed-field gradient NMR measurements have been carried out elsewhere on $LiBF_4$/PC systems for both liquids and polymer gel electrolytes[10, 11]; however usually covering many samples over a small number of concentrations and temperatures.

Dielectric spectroscopy has been employed to measure the ionic conductivity of the liquid electrolytes. The ionic conductivity of an electrolyte is of scientific interest due to the primary application of these solutions as electrochemical devices; which require high conductivities to adequately perform. Detailed research into liquid electrolytes containing $LiBF_4$ have been measured elsewhere with carbonated solvents such as propylene carbonate and their mixtures [12, 13, 14, 15]. In these papers many salt concentrations and temperatures have been probed and have a main emphasis on covering a large range of solvent mixtures. In the research presented here a single salt and solvent system was chosen in order to understand the core principals of the dynamics of the individual constituents. It should also be noted that in this research a conductivity cell was used which are commonly used in solid or gel research. The reason for choosing such a technique was in order to later compare the polymer gel electrolyte conductivity which were measured using the same conductivity cell. This paper will not only consider the conductivity at many different temperatures and salt concentrations, but will compare these results with the diffusion constants which allow a more in depth study of the dynamics and solvation of the ions in solution than previously reported.

Viscosity measurements were also taken at various temperatures and salt concentrations. The viscosity of a liquid electrolyte directly affects the mobility of the ions and therefore the conductivity. The viscosity was measured using a standard Ostwald viscometer which relies on a calibration sample and measured density. The density of the liquid electrolytes was measured alongside the viscosity measurements using several volumetric flasks, which were housed in the same water bath as the viscometer. The

3

use of the viscosity in this research was to determine trends in the average radius of the solvent molecules, lithium cations and fluorinated BF_4 anions. It is also suggested in this research that by fitting a simple exponential to the viscosity and diffusion data as a function of salt concentration that the trends in the effective radii can be determined.

It is commonly known that the ionic conductivity will be affected by the number of charge carriers that form neutral pairs. It is possible by using the Nernst-Einstein equation along with the translational diffusion constants to predict the conductivity; with the assumption that all charge carriers are unpaired and contributing to the conductivity. Therefore by comparing the predicted and measured conductivities it was possible to give an estimation of the degree of ionic association in the liquid electrolytes. Other methods have been employed to probe the ion-ion interactions such as Raman spectroscopy as well as using the Walden product and limiting molar conductivities [16, 17], however the use of the Nernst-Einstein equation to predict conductivity was been proven to be effective for both liquid electrolytes [18, 19, 20, 21, 22, 23] and polymer gel electrolytes[24, 25, 26, 27] and has been shown to yield a good approximation of the ionic interactions.

2. Experimental

2.1. Sample Preparation

All samples were prepared in an oxygen-free nitrogen filled glove box. The liquid electrolytes were prepared by mixing $LiBF_4$ salt with PC solvent at molar concentrations of 0.1-1.5M at room temperature with magnetic stirrer bars. In this study the salt concentration is expressed as salt molality rather than molarity; as molality is independent of temperature. The molar concentrations of 0.1-1.5M corresponds to molal concentrations in the range of 0.08-1.37 mol kg^{-1}. The PC used was 99.7% anhydrous, both the PC and $LiBF_4$ were vacuum sealed from Sigma-Adrich. The liquid electrolyte samples for the NMR diffusion measurements were sealed into 10 mm glass tubes for the ^{19}F and ^7Li measurements and 5 mm glass tubes for the ^1H measurements. The tubes were sealed in the nitrogen atmosphere of the glovebox to avoid any moisture in the samples.

The conductivity samples were also sealed inside the cell while in the glovebox, to reduce the chance of any moisture entering the system. While inside the Novocontrol BS1200 conductivity rig there was a constant supply of nitrogen gas which kept the

4

sample in a nitrogen atmosphere during measurements. Some preliminary measurements were taken for liquid samples that were left in the cell for extended periods of time before being measured; these measurements yielded the same results and therefore it was assumed that moisture in the atmosphere was not affecting the sample.

2.2. NMR Diffusion

NMR diffusion previously measured at Leeds [25] used a Stejskal-Tanner pulse sequence. Here the NMR pulse sequence used was a complex bipolar stimulated echo pulsed-field gradient (BPStE-PFG) originally designed by Cotts [28]. Cotts sequence was an adapted form of a Stejskal-Tanner pulse sequence which eliminates background magnetic fields and has been used here at Leeds in previous studies [8].

Background magnetic field gradients manifest due to inhomogeneities in the magnetic field. The use of bipolar pulses removes these background magnetic field gradients. This introduces the relation for intensity of signal in the form of;

$$I = I_0 \exp\left(-4\pi^2\gamma^2\delta^2 G^2 D \left(\Delta - \frac{\delta}{3}\right)\right) \tag{1}$$

where G is the gradient field strength, Δ is the time between subsequent gradient pulses, δ is the gradient pulse duration and D is the self diffusion coefficient. The NMR parameters used were Δ=40 ms, δ=10 ms and the time between radio frequency (rf) and gradient pulses was 1 ms [25]; these values were unchanged throughout the experiments. The diffusion experiments are two dimensional as they are performed multiple times each with a different value for the pulsed-field gradient strength G. As the gradient is increased the intensity would decrease and therefore by fitting equation 1 to the decay of intensity as a function of gradient strength the diffusion constants were determined. The software that was used was Bruker Topspin 1.5, this software contains a function that calculates the maximum gradient strength to be used depending on the value of the diffusion constant being measured. Between the application of each of the various gradient strengths a time was left in order for the magnetisation from the previous run to dissipate. This delay is known as the recycle delay and was set here to $5T_1$.

The three different nuclei used here were ^{1}H, ^{7}Li and ^{19}F which correspond to the solvent molecules, cations and anions, respectively. The diffusion coefficients were measured using a 400 MHz Bruker AVANCE II Ultrashield NMR spectrometer. All diffusion

5

measurements were carried out using a Diff60 probe supplied by Bruker. Three resonant frequencies used were 400 MHz, 155 MHz and 376 MHz for the ^{1}H, ^{7}Li and ^{19}F nuclei, respectively. The 90° pulse durations were measured using an inbuilt software function of Bruker Topspin 1.5 which was used as an interface for the diffusion measurements. The pulse durations used were determined to be 6.6 μs at a power level of 0 dB, 15.4 μs and 19.6 μs at a power level of 3 dB for the ^{1}H, ^{7}Li and ^{19}F, respectively.

The fitting of the equation 1 has been carried out using Bruker topspin1.5 software which utilises an iterative process based on the Levenberg-Marquardt algorithm [29, 30], in each case the integrated intensities were used.

2.3. Ionic Conductivity

Electrical conductivity has two contributing factors, the conductivity of the ions within the liquid electrolytes (ionic conductivity) and the conductivity arising from the movement of electrons (electronic conductivity). The liquid electrolytes are dominated by the ionic conductivity here making the electronic conductivity negligible. Therefore the term conductivity was synonymous with ionic conductivity in these liquid electrolytes. The conductivity is defined as the inverse of the resistivity of the sample and was determined by using;

$$\sigma = \frac{1}{\rho} = \frac{d}{AR_s} \qquad (2)$$

where σ is the ionic conductivity, ρ is the resistivity of the solution, d is the thickness of the sample, A is the cross-sectional area of the electrodes and R_s is the bulk resistance of the sample. The bulk resistance was taken as the real impedance at the point where the imaginary impedance was zero. The conductivity cell used had a cross sectional area of (0.975 ± 0.009) cm^2 and a thickness of (2.01 ± 0.02) mm. Therefore the cell constant used for all measurements was given by the ratio of d/A of (0.22 ± 0.01) cm^{-1}.

Conductivity measurements were taken with a Novocontrol Alpha Beta frequency analyser which was connected to a modified BDS1200 Novocontrol conductivity rig. The conductivity cells were custom built and consisted of two stainless steel electrodes with polytetrafluoroethylene (PTFE) spacers; PTFE was chosen as the spacer as it is inert and has a very high melting temperature. The cells were made using inert stainless steel blocking electrodes prohibiting the lithium ions from chemically reacting with the

6

electrodes. An alternating current (AC) was applied to the cell by the Novocontrol analyser in the frequency range of 1-10^7 Hz. The total impedance of the conductivity cell is given by;

$$Z_{Cell} = \left[\frac{R_s}{1 + (\omega C_s R_s)^2} \right] - i \left[\frac{\omega C_s R_s^2}{1 + (\omega C_s R_s)^2} + \frac{1}{\omega C_{dl}} \right] \tag{3}$$

where C_s is the capacitance of the electrolyte, C_{dl} is the capacitive term from the electrodes (or double layer), ω is the frequency of the AC signal and i denotes the imaginary term of the impedance. When $\omega C_s << R_s$ the total impedance of the cell can be reduced to;

$$Z_{Cell} \approx R_s - \frac{i}{\omega C_{dl}} \tag{4}$$

therefore the real part of the impedance was equal to the bulk resistance of the sample when the imaginary impedance was zero. In order to determine the point at which this occurs Cole-Cole (Nyquist) plots were used.

The temperature of the sample was maintained by a flow of nitrogen gas through with a 400 W heater. The heater was monitored and controlled by a Eurotherm thermostat. In this research each sample was sealed inside the conductivity cell and all temperatures were measured consecutively from low temperature (253 K) to high temperature (353 K). Each sample was repeated a minimum of three times in order to obtain an average with an uncertainty which indicates the reproducibility of the measurements. It was found that between repeat readings the variance was no more than 2%.

2.4. Viscosity

The viscosity of the liquid electrolytes were measured at different temperatures and salt concentration using a standard Ostwald viscometer ('U' tube). The temperature was controlled via a water bath placed on a hotplate operated by a thermocouple and Eurotherm thermostat. This method limited the temperature range of 293-333 K. Two thermocouples were placed inside the water bath in order to ensure there was no temperature gradient. One was placed at the bottom of the bath and was connected to the thermostat, the other at the top which was used as a reference temperature. In addition a mechanical stirrer was placed in the bath in an attempt to keep the temperature of the bath homogeneous. At all times the two thermocouples were within 0.5 K of each other.

7

A calibration sample was used in order to to eliminate the need for geometrical constants, the ratio of the viscosities is given by:

$$\frac{\eta_{Sample}}{\eta_{Calibration}} = \frac{t_{Sample}\rho_{Sample}}{t_{Calibration}\rho_{Calibration}} \tag{5}$$

where ρ_{Sample} and $\rho_{Calibration}$ are the densities of the sample solution and calibration solution, respectively and t_{Sample} and $t_{Calibration}$ are the time taken to fall a given length through the tube in each instance. Here pure PC was used as the calibration liquid as it has been well characterised elsewhere [31]. Only the viscosity of pure PC was used from Barthel et al [31]; the density of the pure PC was measured *in situ*. The density was measured using 10 ml volumetric flasks, these flasks were housed in the same water bath as the viscometer; this was to ensure a systematic temperature between the two measurements. Two different volumetric flasks were placed in the water bath, both containing the same solution; this was to achieve an average and an attempt to reduce the error. In intervals of 10 K the flasks were set at the 10 ml line and weighed. It was found that there was very little difference between the two flasks.

3. Results

3.1. NMR Self Diffusion

Pulsed-field gradient stimulated echo NMR diffusion measurements of liquid electrolytes containing PC/LiBF$_4$ were measured for samples with salt concentration in the range of 0.1-1.5M, which corresponds to molal concentrations in the range 0.08-1.37 mol kg^{-1}. This upper limit was chosen due to the salt reaching saturation. It has been shown that the stimulated echo pulse sequence is a more reliable method of measuring self diffusion than a standard gradient echo sequence [32]. The three resonant frequencies used were for the ^{1}H, ^{7}Li and ^{19}F nuclei in order to track the diffusion of the PC molecules, cation and anion, respectively. When choosing the diffusion time Δ for the self-diffusion measurements the longitudinal relaxation times (T_1) have to be considered. The diffusion times are usually set so that the T_1 values are much longer than the diffusion time. This is to ensure that there is no decay of the signal during the diffusion measurement. However since the pulsed-field gradient stimulated echo pulse sequence was a constant time experiment the value the diffusion time did not have to be much smaller than T_1.

8
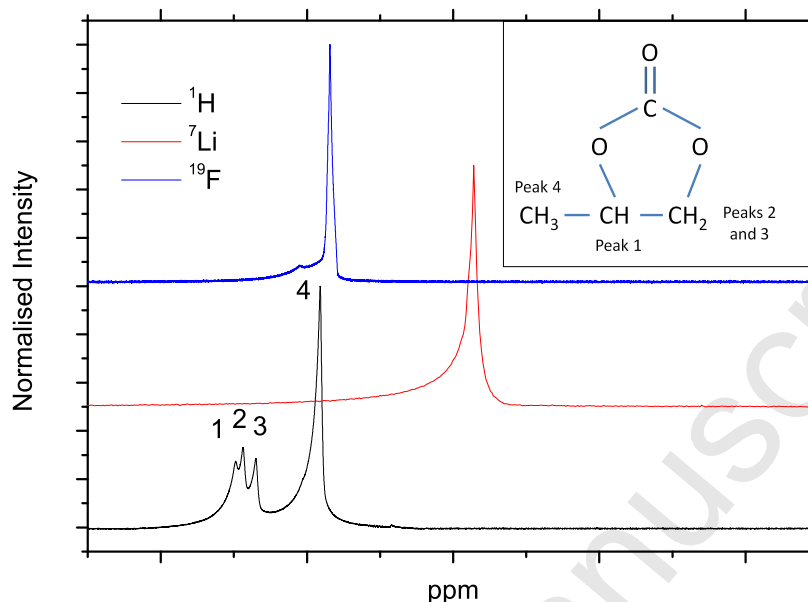
Figure 1: NMR spectra for PC/LiBF$_4$ liquid electrolytes using ^{1}H, ^{7}Li and ^{19}F. The ^{1}H and ^{7}Li spectra are for PC/LiBF$_4$ (0.89 mol kg^{-1}) and PC/LiBF$_4$ (0.61 mol kg^{-1}) for the ^{19}F spectrum. The ^{1}H, ^{7}Li and ^{19}F nuclei were used to measure diffusion of PC molecules, lithium cation and fluorinated anion respectively. All spectra taken at 303 K. Arbitrary chemical shift reference was used. Inset shows structure of propylene carbonate (PC).

If the diffusion time was too long (i.e. 2-3T_1) then the signal would decay too much and therefore the signal to noise ratio (SNR) would be too large. The longitudinal relaxation times were measured for this system elsewhere[9] and found to be of the order of seconds. The diffusion time used here was 40 ms, which is two orders of magnitude smaller, therefore no decay occurred during the diffusion measurements and the SNR was observed to be very good.

Typical spectra for each nuclei are displayed in figure 1 which shows the NMR spectra for PC/LiBF$_4$ (0.89 mol kg^{-1}) for the hydrogen and lithium nuclei and PC/LiBF$_4$ (0.61 mol kg^{-1}) for the fluorine nucleus. The fluorine and lithium spectra exhibited a single peak in the NMR spectra. There was a slight shoulder to some of the fluorine spectra however this was attributed to the shimming. The hydrogen spectrum which was essentially the NMR spectrum for the propylene carbonate molecule exhibited four peaks. The four peaks were attributed to the various hydrogen sites on the molecule. The inset to figure

9

1 shows the structure of the propylene carbonate molecule which has a C-H, a C-H$_2$ and a C-H$_3$ bond attached the the ring. The four peaks of the NMR spectra are attributed to these different hydrogen sites. The peaks have been denoted 1-4 where peak 1 represents the C-H bond, peaks 2 and 3 represent the C-H$_2$ and peak 4 represents the C-H$_3$ bond. Peak 4 exhibited a much higher intensity than the other peaks, this was attributed to the C-H$_3$ bond having three times the number of hydrogen atoms than the other sites.

The diffusion for the hydrogen nucleus was determined from the area of the spectrum as a function of gradient strength (G), the entire spectrum was used. However clearly it is possible to also determine the diffusion of each of the peaks of the hydrogen spectrum. The diffusion measurements of each peak were found to be very similar within error of each other. Taking for example a PC/LiBF$_4$ (0.89 mol kg^{-1}) liquid electrolyte at 293 K the values of diffusion were (2.07 ± 0.02), (2.06 ± 0.02), (2.06 ± 0.02) and (2.06 ± 0.01) (10^{-10} m^2 s^{-1}) for peaks 1-4 of the PC molecule, respectively. The largest deviance between peaks was observed at higher temperatures, however, the deviance was around 0.5% at maximum. The intensity was used to fit the peaks as there was some overlap of peaks 1-3 and therefore an area fit would contain contributions of the neighboring peaks. When fitting the spectrum as a whole the area was more reliable as the strongest peak (peak 4) would overpower the others in an intensity fit.

The diffusion coefficients for the ^{1}H, ^{7}Li and ^{19}F nuclei as a function of salt concentration are shown in figure 2 which represent the PC molecules, lithium cation and fluorinated BF$_4$ anion, respectively. For most salt concentrations the PC molecules were the fastest diffusing entity followed by the BF$_4$ anion then the lithium cations. This is counter-intuitive as the lithium ions are the smallest entity and therefore since all ions and molecules are traveling through the same medium, should exhibit the largest diffusion coefficient. This was attributed to the fact that solvents such as PC which are polar protic, have been found to solvate the cation more favourably than the anion[33]. This is due to the cation having a high charge density which is more attractive than the dispersed charge of the anion. Also the structure of PC contains a carbonyl group (C=O) which protrudes from the ring, containing a small negative charge which will easily bond with the lithium positive charge. This results in the effective radius of the lithium ions being large due to the solvation shell [34]; this diffusion order has been seen

10

1
2
3
4
5
6
7
8
9
10
11
12
13
14
15
16
17
18
19
20
21
22
23
24
25
26
27
28
29
30
31
32
33
34
35
36
37
38
39
40
41
42
43
44
45
46
47
48
49
50
51
52
53
54
55
56
57
58
59
60
61
62
63
64
65
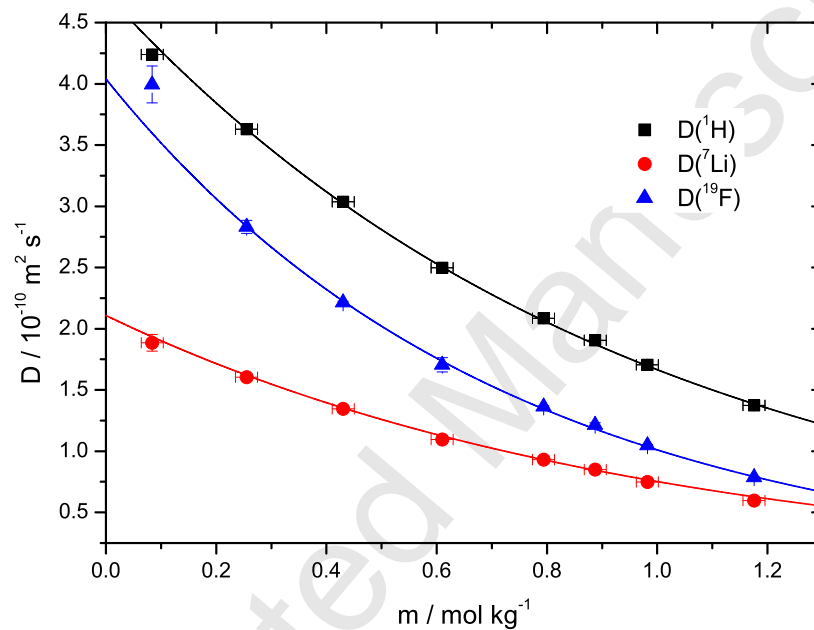
Figure 2: Self diffusion coefficients for PC/LiBF$_4$ liquid electrolytes with increasing salt concentration. All diffusion measurements carried out at 293 K. ^{1}H, ^{7}Li and ^{19}F nuclei are displayed which represent the PC molecules, lithium cation and fluorinated anion (BF$_4$) respectively. The error values for the diffusion were determined from both the fitting of the diffusion decay curve and repeat readings and were of the order 0.05×10^{-10} m^2 s^{-1}. The data has been fitted with equation 6.

11

Temperature / K	D_0 / 10^{-10} m^2 s^{-1}			A_D / mol kg^{-1}		
	^{1}H	^{7}Li	^{19}F	^{1}H	^{7}Li	^{19}F
283	—	1.66	3.08	—	0.87	0.70
293	4.99	2.15	3.95	0.98	0.96	0.75
303	6.23	2.81	4.94	1.07	1.02	0.79
313	7.72	3.50	6.00	1.13	1.08	0.83
323	9.16	4.21	7.30	1.19	1.15	0.86
333	11.6	4.99	9.04	1.15	1.23	0.89
343	12.5	5.91	10.5	1.33	1.33	0.93
353	—	8.26	12.2	—	1.23	0.99

Table 1: Salt concentration fitting parameters A_D and D_0 for diffusion constants for PC/LiBF$_4$ liquid electrolytes using ^{1}H, ^{7}Li and ^{19}F nucleus which represents the solvent molecules, cation and anion respectively.

in many different lithium salts in various other solvents [35, 36, 19, 18, 11]. There are a considerable number of publications on the diffusion of the solvent molecules, cation and anion of lithium based salts in various solvents using this method [18, 19, 11, 37, 21]. With increasing salt concentration the diffusion of the lithium cations and BF$_4$ anions converge; ionic association is the likely cause of such a convergence in the case where the BF$_4$ anions are associating with lithium-solvent clusters. This convergence has been seen elsewhere in a system containing EC:EMC (ethylene carbonate : ethylene methylene carbonate) (2:8) with LiBF$_4$ [38].

The salt concentration dependence of the diffusion measurements were fitted to a simple exponential in the form;

$$D(m) = D_0 exp\left[\frac{m}{A_D}\right] \tag{6}$$

where D_0 is the diffusion at infinite dilution, m is the molal salt concentration and A_D is an exponential fitting parameter. The A_D factor determines the rate at which the diffusion decreases with increasing salt concentration. A smaller value of A_D corresponds to the diffusion decreasing at a faster rate. If the diffusion decrease was caused purely from the increase in viscosity of the system then it would be expected that the A_D values
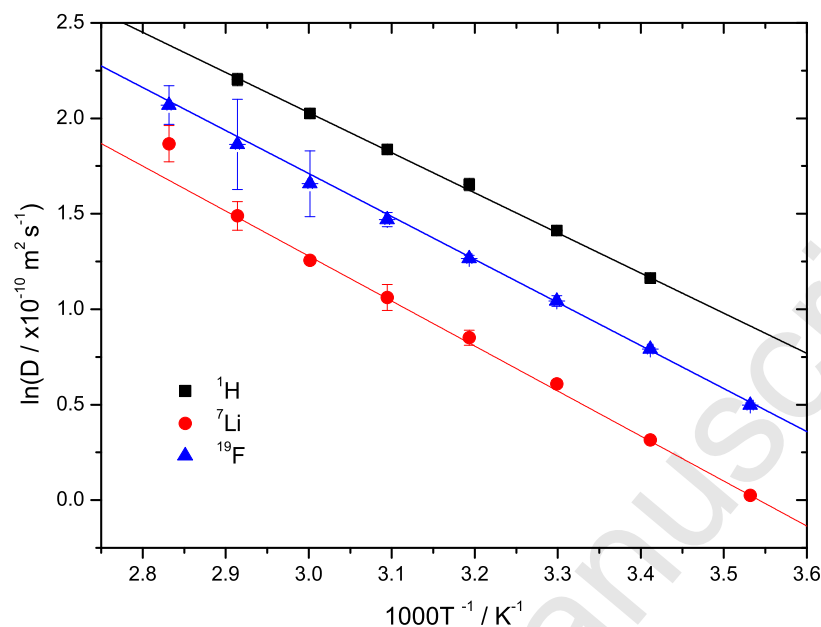
12

Figure 3: Arrhenius plot for self diffusion coefficients for PC/LiBF$_4$(0.43 mol kg^{-1}) liquid electrolyte. Here linear fits have been applied suggesting Arrhenius type temperature dependence. ^{1}H, ^{7}Li and ^{19}F nuclei are displayed which represent the PC molecules, lithium cation and fluorinated anion (BF$_4$) respectively.

would be the same for all nuclei. The parameters of these fits are displayed in table 1. It was observed that the order of the A_D values were ^{1}H > ^{7}Li > ^{19}F, which meant that the fluorine species had the most significant variation with increasing salt concentration. These values can be compared with similar values determined for the viscosity, which is discussed further in section 3.3. All A_D values were observed to increase with increasing temperature which was attributed to the increase in ions to solution.

The temperature range of the diffusion measurements was 293-353 K; the upper limit here was set due to concerns of temperature gradients in the samples at high temperatures which is a known problem in NMR diffusion measurements. A new type of NMR tube has been devised elsewhere [39] to avoid this problem, however here standard NMR tubes were used. Arrhenius plots for the diffusion are shown in figure 3, which involves plotting the natural log of the diffusion values against the inverse of temperature. If the resulting Arrhenius plots can be fitted well with a linear fit then the system is considered to exhibit

13

Arrhenius type temperature dependence. Linear fits have been applied to figure 3, it can be readily observed that the linear line fits the data well, suggesting Arrhenius type dependence of the form;

$$D = D_\infty exp[\frac{E_D}{RT}] \qquad (7)$$

where D_∞ is a diffusion at infinite temperature and E_D is the energy required for the activation of diffusion. VTF type temperature dependence has been seen for other systems with $LiPF_6$ in carbonated solvents ethylene carbonate (EC), dimethyl carbonate (DEC) and propylene carbonate (PC), however this dependence was seen for measurements in a much wider temperature range (233-353 K)[21]. Therefore it was expected that the diffusion values would exhibit VTF type temperature dependence at a larger temperature range. The activation energy E_D shown in figure 4 increased with salt concentration. This is intuitively reasonable as at high salt concentrations the solution is more viscous and hence requires more energy for the ions to translate, therefore increasing the activation energy.

The activation energy of the lithium ions is greater than that of the fluorine, suggesting again that the lithium ions are larger than the fluorine ions, therefore requiring more energy to move through the liquid. However, the activation energies converge at high salt concentrations, supporting the hypothesis that the fluorine and lithium become more associated at high salt concentrations.

3.2. Conductivity

In this section the conductivity results of $LiBF_4$ in propylene carbonate are discussed. Propylene carbonate is a popular choice of solvent both as a single solvent [40] and as part of a multiple solvent system[41, 14, 15, 42] with various, usually lithium based salts. Conductivity measurements of $PC/LiBF_4$ solutions have been measured previously elsewhere [43, 13], however in this paper the conductivity measurements will be used along with the diffusion measurements to determine the ionic association of the solution. In the previous publication of the conductivity behaviour of $PC/LiBF_4$ solutions [43, 13], the conductivity was determined using an LCR meter with an overall accuracy of 0.5% quoted. It should be noted that the conductivity measurements were in good agreement with the measurements taken previously[43, 13]. Ding has previously measured the conductivity of a $PC/LiBF_4$ (0.2863 mol kg^{-1}) liquid electrolyte at 292.5 K as 2.976 mS cm^{-1}

14
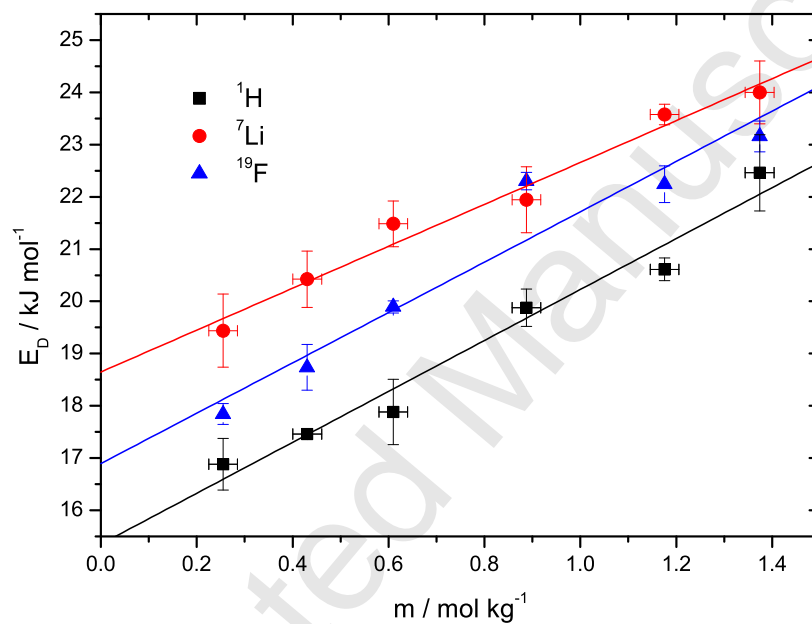
Figure 4: Activation energies for self diffusion coefficients for PC/LiBF$_4$ liquid electrolytes for ^{1}H, [7]Li and ^{19}F nuclei are displayed which represent the PC molecules, lithium cation and fluorinated anion (BF$_4$) respectively. The errors included were determined from the fitting of the Arrhenius equation to the data and were found to be the order of 0.1 kJ mol^{-1}. All data was fitted with linear lines.

15

[43], comparing this value to the closest possible value measured here of PC/LiBF$_4$ (0.26 mol kg^{-1}) at 293 K gave (2.77±0.03) mS cm^{-1}. In the same publication the conductivity of a PC/LiBF$_4$ (0.8373 mol kg^{-1}) liquid electrolyte at 292.5 K was 3.134 mS cm^{-1} [43], again comparing this value to the closest possible value measured here of PC/LiBF$_4$ (0.89 mol kg^{-1}) at 293 K gave (3.03±0.03) mS cm^{-1}. Therefore both of these examples show that the data measured here are in good agreeement with those measured earlier, with the slight discrepancies being attributted to the difference in salt concentration and temperature.

Conductivity measurements were carried out over a temperature range of 253-353 K in 10 K intervals. A frequency range of 1-10^7 Hz was used in these measurements. A Cole-Cole plot was used to determine the point at which the imaginary impedance was zero. The high frequency semi-circles normally characteristic of a Cole-Cole plot were absent in this research due to the conductive nature of the electrolytes studied. However the high frequency end of the semi-circle along with the linear diffusive layer response was present. The bulk resistance of the sample that was used in equation 2 was determined as the real impedance when the imaginary impedance was zero on the Cole-Cole plot.

The temperature dependence of the conductivity was determined in the same manner as the diffusion, Arrhenius plots for PC/LiBF$_4$ (0.08, 0.89 and 1.18 mol kg^{-1}) liquid electrolytes are shown in figure 5. Both linear (dashed) and non-linear (solid) fits were applied and it has been determined that the non-linear Vogel-Tamman-Fulcher (VTF) type dependence is the optimum fit for the conductivity data in the form;

$$\sigma(T) = \sigma_0 exp[\frac{-E'_\sigma}{R(T - T_0)}] \tag{8}$$

where the pre-exponential factor σ_0 is thought to be related to the number of charge carriers [44], E'_σ is a temperature dependent energy term which is dependent on the free energy barrier opposing mobility and T_0 is the ideal glass transition temperature. The values of these parameters have been determined for varying salt concentration of LiBF$_4$. The ionic conductivities of liquid electrolytes are commonly seen to exhibit VTF type temperature dependence [19, 45].

It was found that the value of T_0 was independent of salt concentration, so was set to the average value of 155 K. This was in agreement with work previously reported that showed that T_0 is independent of salt concentration in systems containing poly(ethylene

16
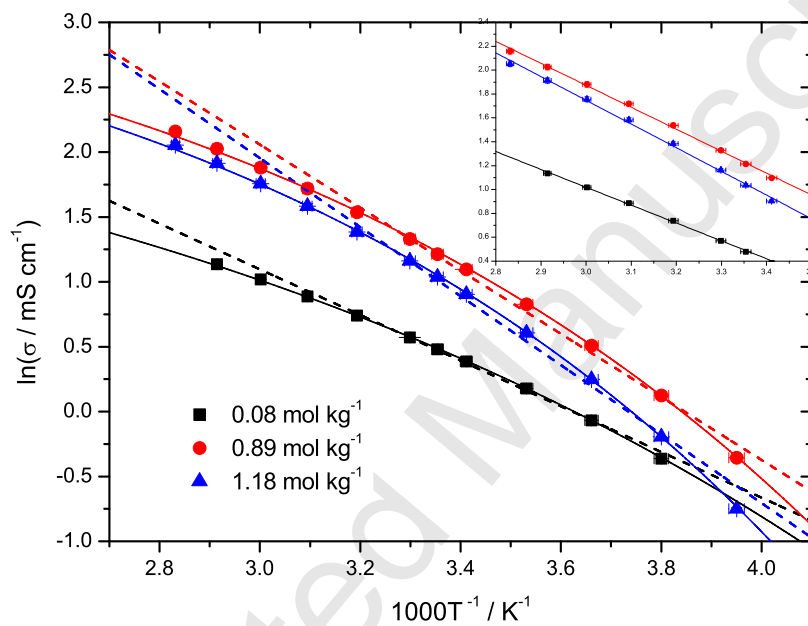
Figure 5: Arrhenius plot for conductivity data of PC/LiBF$_4$ (0.08, 0.89 and 1.18 mol kg^{-1}) liquid electrolytes. Both linear (dashed) and non-linear (solid) fits have been used here, where the linear fit represents Arrhenius type behaviour and non-linear fit (equation 8) represents a VTF type temperature dependence. The errors included here were seen to be around 2% due to very reproducible data between repeat readings. Inset shows the reduced temperature range Arrhenius type behaviour of the liquid electrolytes.

17

glycol) with $LiCF_3SO_3$, $LiClO_4$, $NaClO_4$, $LiBF_4$ and $NaBF_4$ [44]. Figure 6 shows that the activation energy of the conduction mechanism increases with increasing salt concentration; attributed to the ions requiring more energy as the liquid becomes more viscous. The value of σ_0 was seen to increase with salt concentration and this is attributed to the increase in the number of ions in solution.

It would be reasonable to assume that if the diffusion measurements exhibited Arrhenius type temperature dependence that the conductivity would exhibit similar temperature dependence. The conductivity measurements covered a temperature range of 253-353 K, where as the diffusion measurements were limited to 293-353 K. Non-Arrhenius type temperature dependence is usually seen at temperatures near to the glass transition temperature of the sample. Therefore the diffusion temperature dependence was assumed to be Arrhenius at the temperature range measured, however would likely be non-Arrhenius at lower temperatures. In order to compare the activation energies of the diffusion and conductivity, the temperature range of the conductivity was analysed with a reduced temperature range of 293-353 K. The inset of figure 5 shows Arrhenius plots for the reduced temperature range for $PC/LiBF_4$ (0.08, 0.89 and 1.18 mol kg^{-1}) liquid electrolytes. It should be noted that for the temperature range 293-353 K the conductivity data Arrhenius type temperature dependence and therefore the diffusion data was assumed to be Arrhenius due to the limited temperature range. Arrhenius type temperature dependence when in the temperature range 298-343 K has been witnessed elsewhere for a different liquid electrolyte [46]. Similar to the diffusion Arrhenius fitting the conductivity data was fitted to an Arrhenius equation of the form;

$$\sigma(T) = \sigma_\infty exp[\frac{E_\sigma}{RT}] \qquad (9)$$

where σ_∞ is the conductivity at infinite temperature and E_σ is the activation energy of the ionic conduction. The activation energies of the VTF fits and the reduced temperature Arrhenius fits are shown in figure 6 which shows that the activation energy increases with salt concentration for both fitting procedures. The activation energies were seen to exhibit a linear relationship with salt concentration much like the activation energies of the diffusion constants. The activation energies of the Arrhenius fits were all seen to be larger than the corresponding VTF activation energies. This result was reasonably intuitive from simply observing the equations as the VTF equation is scaled by the ideal
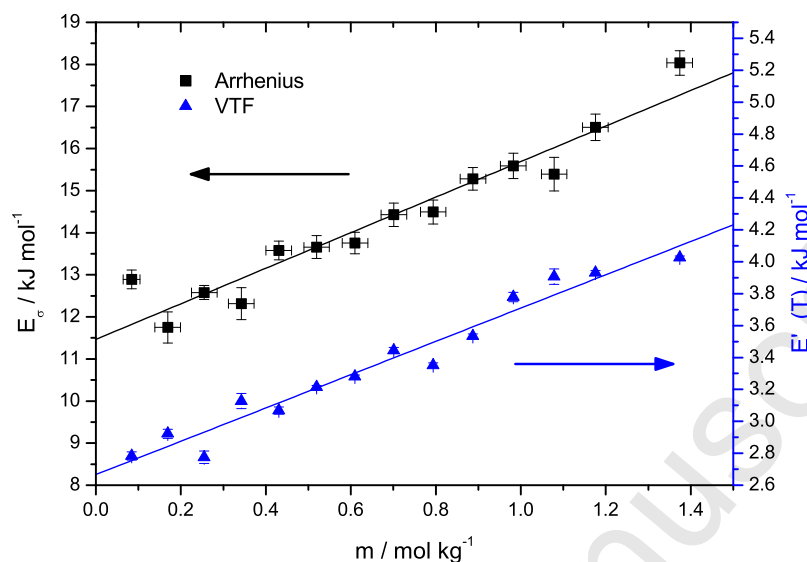
18

1
2
3
4
5
6
7
8
9
10
11
12
13
14
15
16
17
18
19
20
21
22
23
24
25

Figure 6: VTF energy term (E'_σ) and Arrhenius activation energy (E_σ) for reduced temperature range (293-353 K) for conductivity measurements of PC/LiBF$_4$ liquid electrolytes. For the VTF energy term T_0 was held constant for at 155K for all fits.

glass transition temperature.

Figure 7 shows the conductivity of liquid electrolytes as a function of salt concentration for PC/LiBF$_4$ at 253 K, 293 K, 313 K and 333 K. Analysis of figure 7 clearly shows that the conductivity increases with increasing salt concentration at low salt concentrations, then above a critical salt concentration the ionic conductivity begins to decrease. The peak was attributed to a competition between number of ions added to solution, viscosity and ionic association of the solution. Increasing the salt concentration introduces more charge carriers into the solution, however, viscosity of the solution also increases hindering the motion of the ions. The ionic association is defined as the measure of how many of the salt ions added to the solution are free for conduction. The balance between these factors is manifested as a broad peak in conductivity with salt concentration; seen commonly in other systems[13]. Aihara et al [47] have measured the conductivity of PC/LiBF$_4$ liquid electrolytes at 1.0M of salt at room temperature (293 K). They found the conductivity to be around 3.0 mS cm^{-1} which was in very good agreement with the value obtained here of (3.00 ± 0.06) mS cm^{-1}. The black linear line shown in figure 7 was

19

1
2
3
4
5
6
7
8
9
10
11
12
13
14
15
16
17
18
19
20
21
22
23
24
25
26
27
28
29
30
31
32
33
34
35
36
37
38
39
40
41
42
43
44
45
46
47
48
49
50
51
52
53
54
55
56
57
58
59
60
61
62
63
64
65
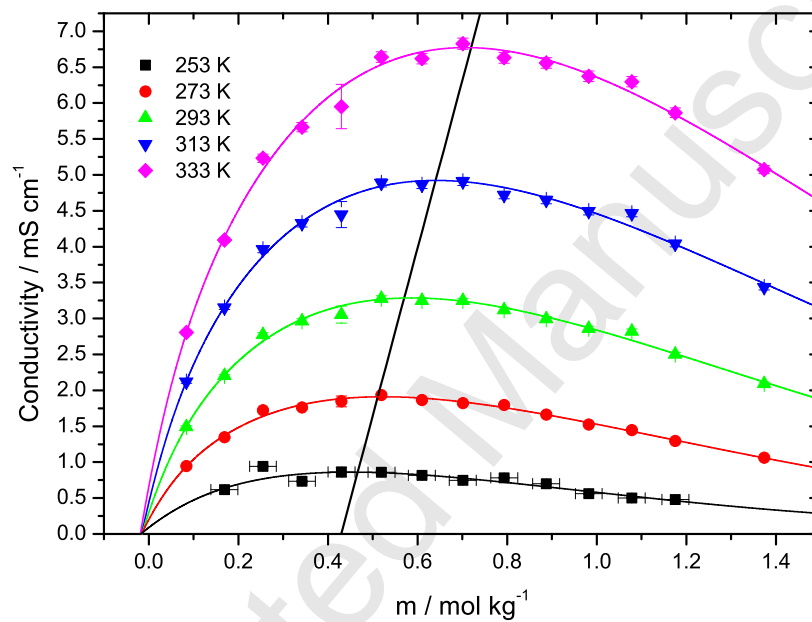
Figure 7: Conductivity for PC/LiBF$_4$ liquid electrolytes against salt concentration. Measurements shown taken at 253 K, 293 K, 313 K and 333 K for all salt concentrations. Casteel-Amis (equation 10) fits have been employed to the data (solid lines). The linear black line has been included to highlight the shift in the position of the maximum with temperature. Error in salt concentration taken as 0.02 mol kg^{-1} which was determined as the most reliable the samples could be produced.

20

the fitted through the position of the maximum for each temperature. It can be readily noted that the linear line had a positive gradient suggesting that the position of the peak shifted with increasing temperature, this has been discussed further in the discussion section.

The Casteel-Amis equation[48] was used to fit the data in Figure 7 and has the form,

$$\sigma(m) = \sigma_{Max} \frac{m}{m_{Max}}^a exp\left\{ b\left(m - m_{Max}\right)^2 - \frac{a}{m_{Max}}\left(m - m_{Max}\right)\right\} \quad (10)$$

where m is the salt concentration in molality, σ_{Max} is the maximum conductivity at any given temperature, m_{Max} is the salt concentration at which the conductivis is at a maximum and a and b are fitting parameters. The Casteel-Amis equation is a semi-empirical equation which is commonly used for determining the salt concentration dependence of liquid electrolytes[49, 50, 51]. A Casteel-Amis plot is shown in figure 8 where the conductivity and salt concentration have been normalised by using the value of σ_{Max} and m_{Max} for each temperature respectively. Casteel-Amis plots have been prepared to show that the conduction mechanism in the liquid electrolyte is unchanged with both increasing temperature and salt concentration. All of the curves overlap suggesting that the ions are conducting in the same manner regardless of temperature and concentration.

3.3. Viscosity

Viscosity measurements have been taken for PC/LiBF$_4$ liquid electrolytes at salt concentrations in the range of 0.08-1.37 mol kg^{-1} at temperatures between 298-333 K. The viscosity in figure 9 was seen to increase with salt concentration. This trend was expected as the more salt introduced to the system the more it will impede the flow of the ions. The rise in temperature gives more energy towards activation and therefore allows higher mobility of the ions. The salt concentration dependence is classically characterised by the Jones and Dole equation[52];

$$\frac{\eta}{\eta_0} = 1 + A\sqrt{c} + Bc \quad (11)$$

where η is the bulk viscosity of the system, η_0 is the viscosity of the pure solvent in this case PC, c is the concentration of the salt in the solution and A and B are fitting parameters. A is related to the mobility and interactions of the ions in solution and B
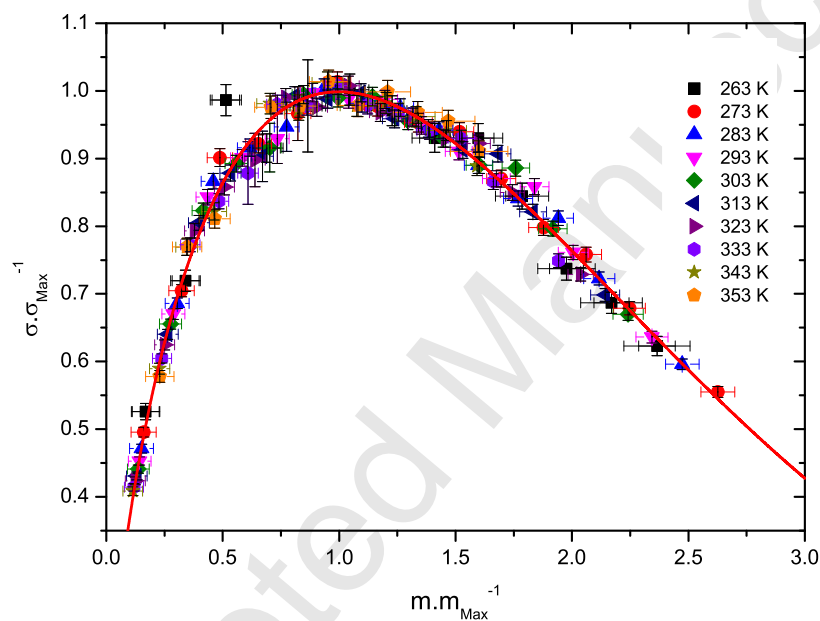
21

Figure 8: Casteel-Amis plot for PC/LiBF$_4$ liquid electrolytes, normalised for relevant maximum values. Temperature taken from 253 K to 353 K for all salt concentrations. Casteel-Amis (equation 10) was fitted to all data (solid line).
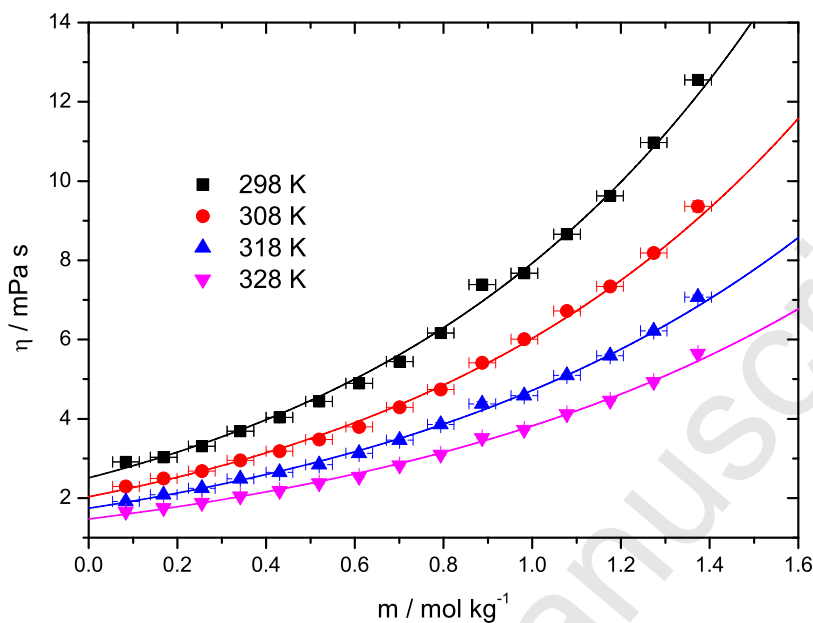
22

1
2
3
4
5
6
7
8
9
10
11
12
13
14
15
16
17
18
19
20
21
22
23
24
25
26
27

Figure 9: Viscosity against salt concentration for liquid electrolytes containing PC/LiBF$_4$ at various temperatures. The data has been fitted with a simple exponential of the form of equation 13.

is related to the interactions between the ions and solvent molecules[53]. Equation 11 is only valid for salt concentrations $c <$ 0.1M [54] and therefore cannot be used here.

For electrolytes at higher salt concentrations it has been shown that adding extra terms at higher orders of magnitude were introduced to allow fitting of these concentrations. Jones and Talley [55], Kaminsky [56] among others introduced a quadratic term to equation 11 in the form;

$$\frac{\eta}{\eta_0} = 1 + A\sqrt{c} + Bc + Dc^2 \tag{12}$$

where the Dc^2 term includes all solute-solvent and solute-solute interactions that were previously unaccounted for in equations 11. The concentration range for this equation is $c <$ 0.2M; which again is too limited for this system. There are also many other empirical fits to salt concentration dependence of the viscosity data of liquid electrolytes including equations by Vand, Afzal, Othmer, Kestin, Klugman, Feldenkamp and Einstein a summary of which is in references [57] and [58]. In this research it was found that the

23

Temperature / K	A_η / mol kg^{-1}	η_0 / mPa s	
		Extrapolated	Measured
298	0.86	2.49	2.51
303	0.88	2.26	2.28
308	0.91	2.02	2.08
313	0.96	1.88	1.91
318	1.00	1.74	1.75
323	1.02	1.59	1.62
328	1.05	1.47	1.50
333	1.09	1.38	1.40

Table 2: Viscosity salt concentration fitting parameters A_η and viscosity of pure PC (η_0) for PC/LiBF$_4$ liquid electrolytes. Both extrapolated η_0 values and those measured by Barthel *et al* are included [31].

best fit was a simple exponential of the form;

$$\eta(m) = \eta_0 exp\left[\frac{m}{A_\eta}\right] \tag{13}$$

where η_0 is the viscosity of the pure solvent, m is the molal salt concentration and A_η is a fitting constant. This equation was the same form as the diffusion salt concentration equation (equation 6); the salt concentration fitting parameters are displayed in table 2. The extrapolated pure solvent viscosity was comparable to the measured viscosity measured elsewhere [31] suggesting that fit was valid. By comparing A_η with the earlier discussed A_D for the diffusion measurements it revealed that for the hydrogen and lithium measurements $A_\eta < A_D$ which means that the diffusion was decreasing at a slower rate than described by the viscosity. This result therefore suggests that the ionic radii of the hydrogen and lithium nuclei decreases with salt concentration. The inverse was observed for the fluorine measurements as $A_\eta > A_D$ which suggests that the diffusion is decreasing at a faster rate than described by the viscosity, suggesting an increase in ionic radii with salt concentration. The A_η parameter was observed to increase with temperature which was attributed to a decrease in the viscosity of the system.

Arrhenius plots of viscosity have been produced in figure 10 and linear fits suggest
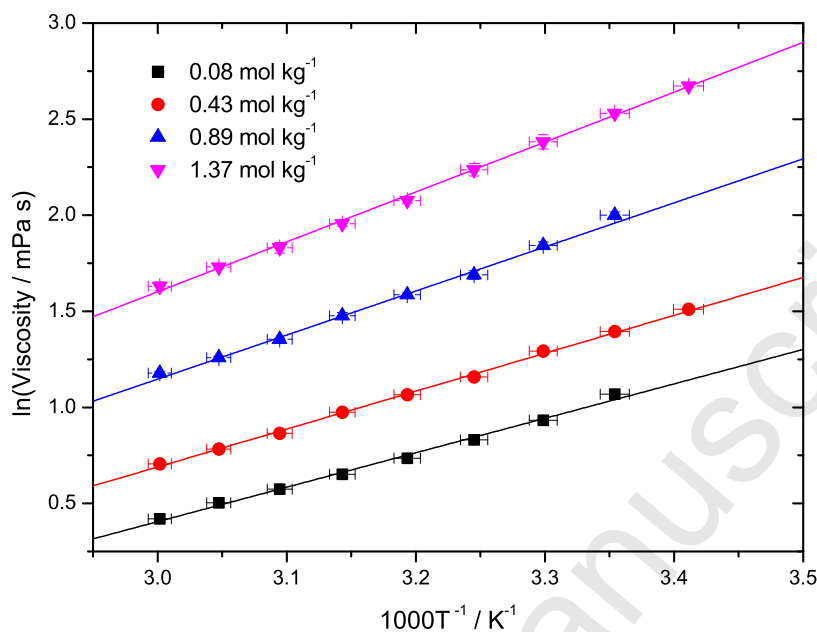
24

Figure 10: Arrhenius plot for PC/LiBF$_4$ liquid electrolyte viscosity. Linear fits have been used here, suggesting that the temperature behaviour is Arrhenius.

Arrhenius type behaviour, expressed via:

$$\eta(T) = \eta_\infty exp[\frac{E_\eta}{RT}] \qquad (14)$$

where η_∞ is the viscosity at infinite temperatures and E_η is the activation energy of the motion of the ions. The viscosity and diffusion have both been shown to display Arrhenius type behaviour, whereas the conductivity exhibits VTF type dependence. The difference in the temperature dependence type was attributed to the larger temperature range of the conductivity measurements, as VTF temperature dependence is usually observed close to the glass transition temperature of the sample. Therefore the diffusion and viscosity measurements were too high to observe the VTF dependence. These trends have been seen elsewhere with different liquid electrolyte systems [59].

4. Discussion

Table 3 shows the activation energies for the diffusion, conductivity and viscosity processes. As with the other processes the activation energy of viscosity increased with

25

increasing salt concentration, which suggests that the energy required for the ions to translate and thus the activation energy increases with salt concentration. In order to compare the different activation energies, the conductivity activation energy was taken as the reduced fit Arrhenius values. The diffusion activation energies at low salt concentration (0.26 mol kg^{-1}) were (16.9 ± 0.5) kJ mol^{-1}, (19.4 ± 0.7) kJ mol^{-1}, (17.8 ± 0.2) kJ mol^{-1} for the ^{1}H, ^{7}Li and ^{19}F nuclei, respectively which suggested that the size order of each nuclei was ^{1}H$<^{19}$F$<^{7}$Li as a larger activation energy suggests a larger radius. It would be expected that the activation energies of the diffusion and viscosity would be comparable as both mechanisms are purely translational, however the diffusion are microscopic measurements and the viscosity measurements are macroscopic. The activation energy of the viscosity for the PC/LiBF$_4$ (0.26 mol kg^{-1}) sample was (15.1 ± 0.1) kJ mol^{-1} which was comparable to the diffusion activation energies. The reduced temperature range conductivity activation energy was (12.6 ± 0.2) kJ mol^{-1} which is lower than the other activation energies. The conductivity was not a purely translational mechanism and therefore it was assumed that the degree of ionic association would affect the activation energy.

The activation energies at high salt concentration (1.37 mol kg^{-1}) were (22.5 ± 0.7) kJ mol^{-1}, (24.0 ± 0.6) kJ mol^{-1}, (23.2 ± 0.3) kJ mol^{-1} for the ^{1}H, ^{7}Li and ^{19}F diffusion, respectively which again suggested a size order of ^{1}H $< ^{19}$F $< ^{7}$Li; this trend was unaffected by salt concentration. It should be noted that the activation energies of the fluorine and lithium nuclei have converged at higher salt concentration suggesting that the fluorine radius has increased. At higher salt concentrations the fluorine was likely associating with the lithium ions, therefore observing a convergence of the activation energies. The activation energy of the viscosity for the PC/LiBF$_4$ (1.37 mol kg^{-1}) sample was (21.6 ± 0.2) kJ mol^{-1} which again was comparable to the diffusion activation energies. The reduced temperature range conductivity activation energy was (18.0 ± 0.3) kJ mol^{-1} which was observed to be lower than the other activation energies. It should be noted that the ratio of conductivity and viscosity activation energies was practically unchanged with salt concentration which suggests that the increase in the activation energy of the conductivity was primarily due to the viscosity. It was also observed that the activation energies of the diffusion and viscosity converged at high salt concentration. The

26

	Activation Energy / kJ mol^{-1}				
	Diffusion				
Salt Conc. / mol kg^{-1}	^{1}H	^{7}Li	^{19}F	Conductivity	Viscosity
0.08	—	—	—	12.9	14.9
0.26	16.9	19.4	17.8	12.6	15.1
0.43	17.5	20.4	18.7	13.6	16.4
0.61	17.9	21.5	19.9	13.8	17.5
0.89	19.9	21.9	22.3	15.3	19.1
1.18	20.6	23.6	22.2	16.5	20.5
1.37	22.5	24.0	23.2	18.0	21.6

Table 3: Activation energies for diffusion constants using ^{1}H, ^{7}Li and ^{19}F nuclei which represents the PC molecule, cation and fluorinated anion (BF$_4$) respectively as well as activation energies of viscosity and reduced temperature range conductivity for PC/LiBF$_4$ liquid electrolytes. All activation energies determined from Arrhenius fitting of the data. The error on the activation energies were all found to be of the order 0.1 kJ mol^{-1}.

conductivity activation energies were within 20% of the viscosity energies, where as the diffusion activation energies of were within 10%, 20% and 15% for the ^{1}H, ^{7}Li and ^{19}F of the viscosity energies respectively.

4.1. Ionic Association

Using the diffusion coefficients of the anion and cation along with the Nernst-Einstein equation (equation 15) a predicted value of conductivity can be determined,

$$\sigma(T) = \frac{nq^2}{k_B T} \left[D\left(^{19}F\right) + D\left(^7Li\right) \right] \tag{15}$$

where n is the number of ions per unit volume of charge q added to the electrolyte. $D(^{19}F)$ and $D(^7Li)$ correspond to the diffusion coefficients of the BF$_4$ anion and lithium cation, respectively; obtained from pulsed-field gradient NMR experiments. Using this equation requires the assumption that there is no association between anion and cation. Therefore the difference between the measured conductivity and that determined from equation 15 is the degree of ionic association can be calculated using:

$$\alpha = \left(1 - \frac{\sigma_{Measured}}{\sigma_{Predicted}} \right) \tag{16}$$
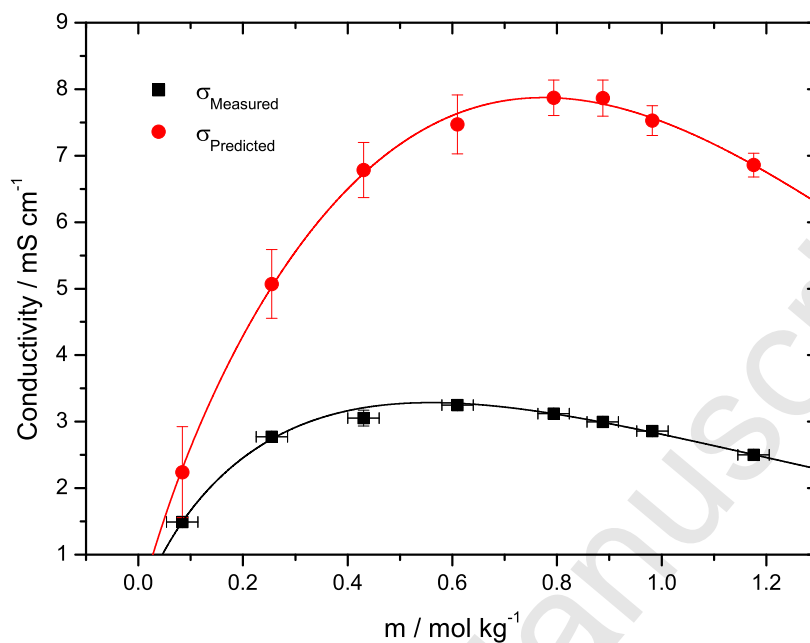
27

Figure 11: Conductivity for both directly measured (square) and predicted (circle) from the Nernst-Einstein equation with salt concentration for PC/LiBF$_4$ at 293 K. Both sets of data were fitted with the Casteel-Amis equation (equation 10).

where α is the degree of ionic association and $\sigma_{Measured}$ and $\sigma_{Predicted}$ refer to the directly measured conductivity and conductivity predicted from equation 15, respectively. Therefore the degree of ionic association is the number of ions which are neutral entities within the liquid electrolyte which do not contribute to the conductivity. The Nernst-Einstein equation is a commonly used tool to determine the level of ionic association (sometimes expressed as the ionic dissociation) for liquid electrolytes[45, 60, 61].

Figure 11 shows the predicted conductivity was significantly higher than the corresponding measured conductivity. It also shows that the predicted conductivity exhibits a peak, but at a significantly higher salt concentration than the measured conductivity. Since the viscosity is the same for each case, this difference has been attributed to ionic association and will be discussed later in section 4.2. Using equation 16 and the ratio of measured and predicted conductivity the ionic association was calculated.

Figure 12 shows the degree of ionic association for these liquid electrolytes as a function of salt concentration. It can be seen that there is an increase of ionic association with

28

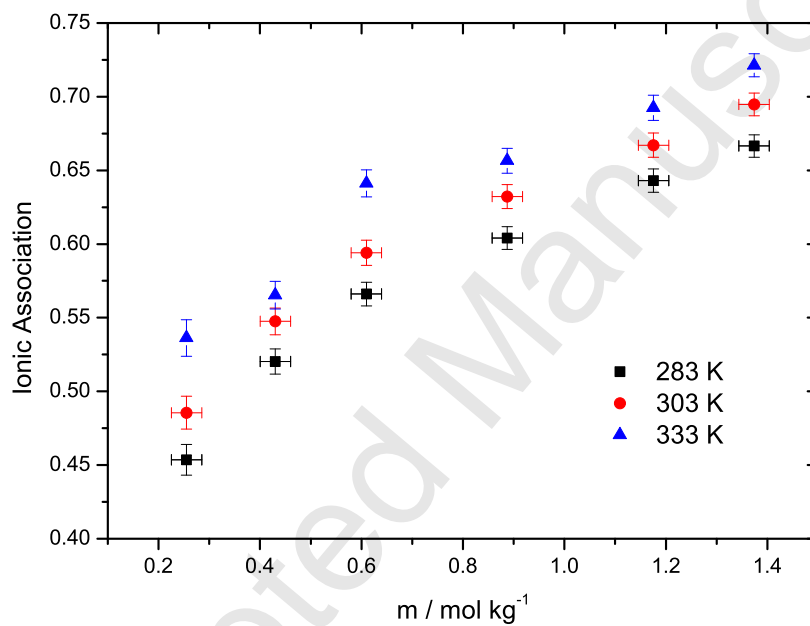Figure 12: Degree of ionic association against salt concentration for PC/LiBF$_4$ at 293 K. Error values were determined from error propagation from the values of diffusion of both the cation and anion as well as the the measured conductivity.

29

Figure 13: Degree of ionic association against temperature for PC/LiBF$_4$ liquid electrolytes. Error values were determined from error propagation from the values of diffusion of both the cation and anion as well as the the measured conductivity. Linear fits have been applied to the data.
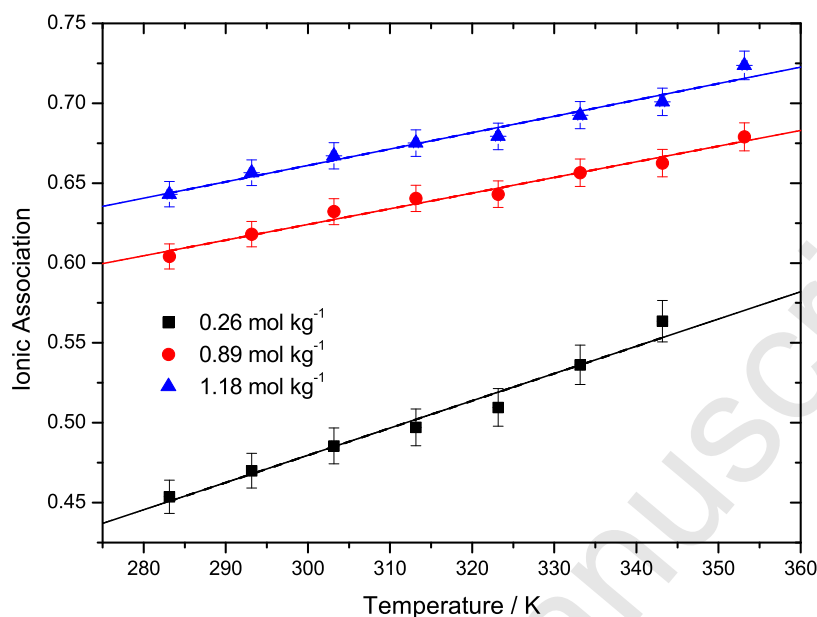
salt concentration, a similar result has been shown for six different lithium based salts with gamma-butyrolactone (GBL) as the solvent [11]. Also highlighted by the Aihara *et al* research (ref [11]) was that the order of association for the six different salts were LiSO$_3$CF$_3$ > LiBF$_4$ > LiBETI $\approx$ LiBOB $\approx$ LiTFSI $\approx$ LiPF$_6$. This suggests that the salt used here (LiBF$_4$) had one of the largest ionic associations of the six salts analysed in their research. The trend with increasing salt concentration was attributed to an increased density of ions, resulting in a decreased inter-ion distance.

The temperature dependence of the ionic association is shown in figure 13, which reveals an increase in the ionic association with temperature. This has been seen in other systems and was attributed to the lowering of free energy of ion pair formation at higher temperatures [25]. This result is somewhat counter intuitive since as the temperature is raised the ions would have more thermal energy and therefore one might expect this to promote ionic dissociation. It has been stated by Olender *et al* [25, 62] that for a chemical reaction such as this, in the form $MA \rightleftharpoons M^+ + A^-$, an equilibrium constant

30

can be defined as:

$$K = exp[-\frac{\Delta G^0}{RT}] \qquad (17)$$

where K is the equilibrium constant, G^0 is the difference between the standard Gibbs free energy of the reactants and the products and T is the absolute temperature. The difference in free energy can be simply expressed as:

$$\Delta G^0 = \Delta H^0 - T\Delta S^0 \qquad (18)$$

where ΔH^0 is the change in enthalpy and ΔS^0 is the change in entropy. The enthalpy can be broken down into two different components, the positive energy term for promoting dissociation of the salt ions and a term dependent on the pressure and volume change due to the reaction. It was stated by Olender et al [62] that the volumetric term of the enthalpy can outweigh the positive energy term and also be negative due to electrostriction. This would allow the ionic association to increase with increasing temperature as observed in this study. It has also been found in research elsewhere that the dielectric constant of a liquid electrolyte can decrease with increasing temperature, which would also increase the ionic association at higher temperatures [63].

4.2. Conductivity Peak Shift

It was shown earlier that a peak in the conductivity was observed with salt concentration. This was attributed to an initial increase in the number of free ions however an inevitable increase in viscosity eventually dominates the system and the conductivity starts to decrease. It was also stated earlier that there was a shift in the position of the peak with increasing temperature. Figure 14 shows the position of the maximum (m_{Max}) as a function of temperature for the predicted and measured conductivity of the liquid electrolytes. The temperature dependence of the m_{Max} parameter has been shown in other liquid systems based on propylene carbonate [64].

It was observed that the predicted conductivity exhibited a much higher peak position (m_{Max}) than the measured conductivity. It was stated earlier that since the only difference between the measured and predicted conductivities is the degree of ionic association, as the predicted conductivity assumed no ionic association. An increase in the ionic association would result in a lowering of the conductivity and therefore a reduction of the position of the maximum (m_{Max}).
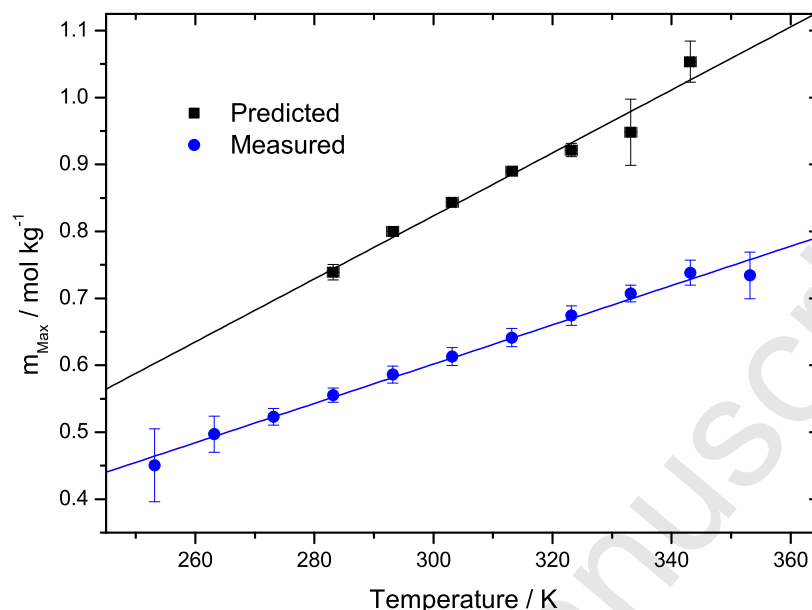
31

Figure 14: Salt concentration at maximum conductivity (m_{Max}) against temperature for PC/LiBF$_4$ liquid electrolytes for both measured and calculated conductivity. The data here has been fitted with linear lines.

4.3. Effective Ion Radius

The Stokes-Einstein equation (equation 19) can be used to calculate a value of the effective radius of the ions. The assumptions of using this equation are that the micro-diffusion relates to the macro-viscosity and also that all of the ion structures are spherical,

$$r = \frac{k_B T}{6c_{SE}\pi D\eta} \tag{19}$$

where r is the effective radius of an ion, k_B is Boltzmann's constant, T is temperature, D is the self diffusion coefficient of the relevant ion, η is the bulk viscosity and $6c_{SE}$ is a factor that is usually between 4 and 6 for a perfect slip boundary and stick boundary, respectively [65]. If c_{SE} takes the value of 1, then equation 19 becomes the classical Stokes-Einstein equation which assumes that the translating object is perfectly spherical; therefore a deviance of c_{SE} away from can indicate a non spherical structure. The c_{SE} parameter for the hydrogen diffusion measurements has been determined empirically by taking a ratio of the known Van der Waals radii and the pure solvent measurements. It has been shown elsewhere that the Van der Waals radius of the PC

32

molecule is 0.276 nm [66]. The average value of the ionic radii measured here for pure PC was (0.153±0.004) nm which is significantly lower due to a deviance from the hard sphere model. By taking a ratio of the measured radius and the radius determined elsewhere yields a correction factor of (0.55±0.01), which agrees with a value of c_{SE} empirically determined elsewhere for PC [35]. The previously determined value of the radius of PC was done so by using molecular mechanics calculations (MM2) [66]. The authors have determined the size of the molecule in three dimensions x, y and z, which they labeled a, b and c, respectively[66]. They go on to say that if there is a difference between the three parameters then the molecule cannot be considered spherical and the best way to determine the deviance is to use c/a. They found that $a=0.781$ and $c=0.430$, which yields a value of the ratio of $c/a=0.55$ for PC[66]; therefore the value obtained elsewhere perfectly coincides with the value measured directly here.

The correction factor for the BF_4 anion has been analysed elsewhere [66], it was shown in that the factor was $c/a=0.89$ and $c/a=0.92$ from crystallographic data and MM2 calculations, respectively. By taking an average of these values it yields $c_{SE}=0.9$. To determine the c_{SE} factor for the lithium cations was more difficult than for the PC molecules; however it has been determined elsewhere and will be used here as 0.95 [66].

The Stokes-Einstein equation is used frequently to calculate the radius using NMR diffusion constants and viscosity measurements [67, 68, 22]. It should be noted that for the ionic radii to be accurately obtained in this way the diffusive species has to much larger than the liquid particles driving the Brownian motion, therefore the values reported here are to show the trends with salt concentration rather than a definitive value of the ionic radius. Using the diffusion and bulk viscosity values the effective radii of the fluorinated BF_4 anion, lithium cation and PC molecules can now be determined.

Table 4 shows the effective radius calculations for the PC molecules, cation and BF_4 anion with increasing salt concentration at 303 K and 323 K. It can be seen from table 4 that the size of the lithium cation is the largest entity, this is due to the cation associating with several solvent molecules [33]. It has been observed elsewhere that on average four PC molecules will associate with a single lithium cation [34]. Since the radius of a single lithium ion is around 0.076 nm [69], it is clear that the lithium ions are solvated by the solvent molecules. It can readily observed from table 4 that the lithium ions decrease in

33

Salt Conc. / mol kg^{-1}	Ionic Radius / 10^{-10} m					
	303 K			323 K		
	PC	Li	BF$_4$	PC	Li	BF$_4$
0.00	2.86	—	—	2.88	—	—
0.26	2.68	3.59	2.26	2.82	3.64	2.30
0.43	2.70	3.49	2.38	2.88	3.63	2.55
0.61	2.65	3.46	2.52	2.86	3.57	2.65
0.89	2.29	3.12	2.44	2.48	3.27	2.66
1.18	2.34	3.10	2.63	2.54	3.23	2.83
1.37	2.14	3.01	2.61	2.37	3.16	2.80

Table 4: Ionic radius calculations for PC molecules, lithium cation and BF$_4$ anion at salt concentrations between 0-1.37 mol kg^{-1} (corresponding to a molarity of 0-1.5M) at 303 K and 323 K.

radius with increasing salt concentration. For the 303 K calculations the lithium radii range from 0.359-0.301 nm from low to high salt concentration. This result was attributed to an increase in ionic association with increasing salt concentrations, as described above. This would therefore mean that as the ionic association increased the lithium cations would partially lose their PC solvation shell in order to associate to the fluorinated BF$_4$ anions. Since the radius calculations are strictly averages of all molecules and clusters contained within the liquid electrolyte, the average effective radius of a lithium cation would decrease since the lithium-fluorine LiBF$_4$ structure is smaller than the solvated lithium one. It has been shown elsewhere that the radius for a lithium ion solvated by four PC molecules is around 0.370 nm [18], this is comparable to the measurements here at low salt concentrations. Therefore it is assumed that at low salt concentrations the ionic association is low and therefore the lithium ions are predominantly solvated by multiple solvent molecules.

The effective radii of the BF$_4$ anion is also displayed in table 4. It can be observed that unlike the lithium ions the effective radii of the BF$_4$ anions increases with salt concentration. This was attributed to the increase in ionic association, as the anion and cation start to associate the size will increase. This also offers an explanation to the convergence of the lithium and fluorine diffusion coefficients shown in figure 2. For the

34

303 K calculations the BF_4 ions were observed to exhibit effective radii in the range 0.226-0.261 nm, from low to high salt concentration. The low salt concentration calculation of 0.226 nm is comparable to the known BF_4 anion radius of 0.229 nm [66]. This therefore has a strong indication that the BF_4 anion does not have a solvation shell like the lithium cation. The increase in size with salt concentration is attributed to the increased ionic association at higher salt concentrations.

The effective radii of the PC molecules (from ^1H NMR measurements) has also been displayed in table 4. Similar to the effective radii of the lithium ions, the PC molecules radii decrease with salt concentration. This agrees with the hypothesis that as the cation and anion associate, the lithium-PC structures are being partially separated in favour of ionic association, therefore resulting in a reduction in the average effective radius of the PC molecules. The lithium, PC and BF_4 radii are relatively unaffected by a change in temperature, which has also been seen in previous work in a system of tetraethylene glycol dimethyl ether (TG) with $LiCF_3SO_3$ [25].

Using this method to calculate the ionic radius can be problematic as it uses micro-diffusion with macro-viscosity. From equation 19 it can be seen that by plotting ln(diffusion) against ln(viscosity) that the gradient should be close to unity if the equation is valid. It was observed that all values of the gradient for all three nuclei were reasonably close to unity, which suggests that it is valid to use the micro-diffusion with the bulk viscosity of the liquid electrolytes. The average gradients over the range of concentrations were (1.05 ± 0.02), (1.12 ± 0.03) and (1.03 ± 0.02) for the ^1H, ^7Li and ^{19}F measurements, respectively. Therefore since all of these values are close to one it can summarised that using the Stokes-Einstein equation can be assumed to give a good to estimation of the effective radii.

5. Conclusions

Pulsed-field gradient diffusion measurements were taken using ^1H, ^7Li and ^{19}F nuclei for $PC/LiBF_4$ liquid electrolytes as a precursor to understanding the conduction mechanism in polymer gel electrolytes. Conductivity and viscosity measurements have also been taken in order to understand the dynamics of the constituents of the solution.

The lithium ion diffusion was found to be slower than the hydrogen and fluorine

35

due to the lithium ion solvating PC molecules resulting in a large effective radius of the lithium species. The diffusion and viscosity measurements both exhibit Arrhenius type behaviour whereas the conductivity displayed VTF temperature dependence. This has been attributed to the extended temperature range of the conductivity measurements which was 253-353 K, where as the viscosity and diffusion were measured using a range of 293-353 K. Therefore the extension to lower temperatures has revealed the VTF type temperature dependence as we are approaching the glass transition temperature.

All liquid electrolytes were seen to exhibit a peak in conductivity with increasing salt concentration. This was attributed to a competition between number of free ions and viscosity. However, with the increase of temperature the peak exhibits a shift to higher salt concentrations. This has been attributed to the lowering of viscosity at high temperatures allowing more salt to be dissolved before viscous effects become the dominating factor; the ionic association is also believed to affect the position of the maximum.

The Nernst-Einstein equation was used to predict conductivity from NMR diffusion coefficient measurements. It was found that the predicted conductivity was significantly larger than the measured values due to the assumption that the anion and cation travel through the medium as dissociated ions. From the difference between the predicted and measured conductivity the degree of ionic association was calculated for the $PC/LiBF_4$ liquid electrolytes. The ionic association was seen to increase with temperature which has been attributed to the lowering of free energy of ion pair formation at higher temperatures. The ionic association also increases with salt concentration and this has been attributed to the increase in ion density in the electrolyte causing more interaction between the anion and cation.

The Stokes-Einstein equation was used to predict the ionic radii of the PC molecules, lithium cation and BF_4 anion. It should be noted that in order to use the Stokes-Einstein equation to calculate the effective radii the radius of the relevant diffusing species has to be significantly larger than the liquid particles driving the Brownian motion. The ionic radii reported here were used to compare the different constituents as well as observing trends with salt concentration. The size order of the constituents were PC molecules, fluorinated BF^4 anion and lithium cations from smallest to largest. The lithium is known

36

to be well solvated, with a large solvation shell. The BF_4 anions and lithium cation were observed to converge at high salt concentration and this was attributed to increased association between the fluorine and lithium. There was no evidence that the BF_4 anions were solvated as the calculated radii were similar to that measured elsewhere for a single BF_4 ion. The effective radii of the PC molecules were also seen to decrease with salt concentration, this is consistent with the hypothesis that the lithium ions are dissociating from the PC molecules in favour of the fluorinated BF_4 anions.

5.1. Acknowledgments

References

[1] P.V. Wright. Recent trends in polymer electrolytes based on poly(ethylene oxide). *Journal of Macromolecular Science-Chemistry*, A26:519–550, 1989.

[2] M. Armand. Polymer solid electrolytes - an overview. *Solid State Ionics*, 9-10:745–754, 1983.

[3] S.A. Dobrowski, G.R. Davies, J.E. McIntyre, and I.M. Ward. Ionic conduction in poly(n,n-dimethyl-acrylamide) gels complexing lithium salts. *Polymer*, 32:2887–2891, 1991.

[4] N. Boden, S.A. Leng, and I.M. Ward. Ionic-conductivity and diffusivity in polyethylene oxide electrolyte-solutions as models for polymer electrolytes. *Solid State Ionics*, 45:261–270, 1991.

[5] A.M. Voice, J. P. Southall, V. Rogers, K. H. Matthews, G. R. Davies, J. E. Mclntyre, and I. M. Ward. Thermoreversible polymer gel electrolytes. *Polymer*, 35 (16):3363–3372, 1994.

[6] I.M. Ward and H.V.St.A. Hubbard. *Polymer electrolytes: conduction mechanisms and battery applications, Chapter 21, in Ionic interactions in natural and synthetic macromolecules.* Wiley and Sons Inc., 2012.

[7] J.E. McIntyre, I.M. Ward, H.V.St.A. Hubbard, and V. Rogers. Uk patent application pct/gb92/01781. 1992.

[8] P.M. Richardson, A.M. Voice, and I.M. Ward. Two distinct lithium diffusive species for polymer gel electrolytes containing LiBF4, propylene carbonate (PC) and PVDF. *The International Journal of Hydrogen Energy*, 39(6):2904Ǔ2908, 2014.

[9] P.M. Richardson, A.M. Voice, and I.M. Ward. Nmr t1 relaxation time measurements and calculations with translational and rotational components for liquid electrolytes containing libf4 and propylene carbonate. 139:214501, 2013.

37

[10] K. Hayamizu, Y. Aihara, S. Arai, and W.S. Price. Self-diffusion coefficients of lithium, anion, polymer, and solvent in polymer gel electrolytes measured using li-7,f-19, and h-1 pulsed-gradient spin-echo nmr. *Electrochimica Acta*, 45:1313–1319, 2000.

[11] Y. Aihara, T. Bando, H. Nakagawa, H. Yoshida, K. Hayamizu, E. Akiba, and W.S. Price. Ion transport properties of six lithium salts dissolved in gamma-butyrolactone studied by self-diffusion and ionic conductivity measurements. *Journal of The Electrochemical Society*, 151(1):A119–A122, 2004.

[12] M.S. Ding. Electrolytic conductivity and glass transition temperatures as functions of salt content, solvent composition, or temperature for libf4 in propylene carbonate plus diethyl carbonate. *Journal of Chemical and Engineering Data*, 49:1102–1109, 2004.

[13] M.S. Ding and T.R. Jow. How conductivities and viscosities of pc-dec and pc-ec solutions of libf4, lipf6, libob, et4nbf4, and et4npf6 differ and why. *Journal of The Electrochemical Society*, 151(12):A2007–A2015, 2004.

[14] G. Moumouzias, G. Ritzoulis, D. Siapkas, and D. Terzidis. Comparative study of LiBF4, Li-AsF6, LiPF6, and LiClO4 as electrolytes in propylene carbonate-diethyl carbonate solutions for Li/LiMn2O4 cells. *Journal of Power Sources*, 122(1):57–66, 2003.

[15] M.S. Ding. Conductivity and viscosity of PC-DEC and PC-EC solutions of LiBF4. *Journal of The Electrochemical Society*, 151(1):A40–A47, 2004.

[16] P.K. Muhuri and D.K. Hazra. Electrical conductances for some tetraalkylammonium bromides, lithium tetrafluoroborate and tetrabutylammonium tetrabutylborate in propylene carbonate at 25 [degree]c. *Journal of the Chemical Society, Faraday Transactions*, 87:3511–3513, 1991.

[17] H. Tsunekawa, A. Narumi, M. Sano, A. Hiwara, M. Fujita, and H. Yokoyama. Solvation and ion association studies of libf4-propylenecarbonate and libf4-propylenecarbonate-trimethyl phosphate solutions. *Journal of Physical Chemistry B*, 107:10962–10966, 2003.

[18] Y. Saito, H. Yamamoto, H. Kageyama, O. Nakamura, T. Miyoshi, and M. Matsuoka. Investigation of the solution condition of lithium electrolyte solutions with LiCF3SO3 salt. *Journal of Materials Science*, 35(4):809–812, 2000.

[19] Y. Aihara, K. Sugimoto, W.S. Price, and K. Hayamizu. Ionic conduction and self-diffusion near infinitesimal concentration in lithium salt-organic solvent electrolytes. *The Journal of Chemical Physics*, 113(5):1981–1991, 2000.

[20] K. Hayamizu and Y. Aihara. Ion and solvent diffusion and ion conduction of PC-DEC and PC-DME binary solvent electrolytes of LiN(SO2CF3)2. *Electrochimica Acta*, 49(20):3397–3402, 2004.

[21] K. Hayamizu. Temperature dependence of self-diffusion coefficients of ions and solvents in ethylene carbonate, propylene carbonate, and diethyl carbonate single solutions and ethylene carbonate + diethyl carbonate binary solutions of LiPF6 studied by NMR. *Journal of Chemical & Engineering Data*, 57(7):2012–2017, 2012.

[22] J.S. Kim, Z. Wu, A.R. Morrow, A. Yethiraj, and A. Yethiraj. Self-diffusion and viscosity in electrolyte solutions. *The Journal of Physical Chemistry B*, 116(39):12007–12013, 2012.

[23] K. Kuratani, N. Uemura, H. Senoh, H.T. Takeshita, and T. Kiyobayashi. Conductivity, viscosity

38

and density of MClO4 (m =ăli and na) dissolved in propylene carbonate and gamma-butyrolactone at high concentrations. *Journal of Power Sources*, 223:175–182, 2013.

[24] H.V. St. A. Hubbard, J.P. Southall, J.M. Cruickshank, G.R. Davies, and I.M. Ward. A comparison of ionic conductivity behaviour in various ethylene oxide based polymer electrolytes. *Electrochimica Acta.*, 43 (10-11):1485–1492, 1998.

[25] M.J. Williamson, J.P. Southall, H.V. St. A. Hubbard, S.F. Johnston, G.R. Davies, and I.M. Ward. Nmr measurements of ionic mobility in model polymer electrolyte solutions. *Electrochimica Acta*, 43 (10-11):1415–1420, 1998.

[26] M.J. Williamson, J.P. Southall, H.V.St.A. Hubbard, G.R. Davies, and I.M. Ward. Pulsed field gradient nmr diffusion measurements on electrolyte solutions containing licf3so3. *Polymer*, 40:3945–3955, 1999.

[27] I.M. Ward, M.J. Williamson, H.V. St.A. Hubbard, J.P. Southall, and G.R. Davies. Nmr studies of ionic mobility in polymer gel electrolytes for advanced lithium batteries. *Journal of Power Sources*, 81-82:700–704, 1999.

[28] R.M. Cotts, M.J.R. Hoch, T. Sun, and J.T. Markert. Pulsed field gradient stimulated echo methods for improved nmr diffusion measurements in heterogeneous systems. *Journal of Magnetic Resonance*, 83:252–266, 1989.

[29] K. Levenberg. A method for the solution of certain non-linear problems in least squares. *Quarterly of Applied Mathematics*, 2:164–168, 1944.

[30] D. Marquardt. An algorithm for least-squares estimation of nonlinear parameters. *SIAM Journal on Applied Mathematics*, 11 (2):431Ű441, 1963.

[31] J. Barthel, R. Neueder, and H. Roch. Density, relative permittivity, and viscosity of propylene carbonate plus dimethoxyethane mixtures from 25 degrees c to 125 degrees c. *Journal of Chemical and Engineering Data*, 45(6):1007–1011, 2000.

[32] G. Annat, D.R. MacFarlane, and M. Forsyth. Transport properties in ionic liquids and ionic liquid mixtures: The challenges of NMR pulsed field gradient diffusion measurements. *The Journal of Physical Chemistry B*, 111(30):9018–9024, 2007.

[33] H.L. Yeager, J.D. Fedyk, and R.J. Parker. Spectroscopic studies of ionic solvation in propylene carbonate. *Journal of Physical Chemistry*, 77 (20):2407–2410, 1973.

[34] H. Ohtani, Y. Hirao, A. Ito, K. Tanaka, and O. Hatozaki. Theoretical study on thermochemistry of solvated lithium-cation with propylene carbonate. *Journal of Thermal Analysis Calorimetry*, 99:139–144, 2010.

[35] Kikuko Hayamizu, Yuichi Aihara, Shigemasa Arai, and Garcia. Pulse-gradient spin-echo 1H, 7Li, and 19F NMR diffusion and ionic conductivity measurements of 14 organic electrolytes containing LiN(SO2CF3)2. *The Journal of Physical Chemistry B*, 103(3):519–524, 1999.

[36] Kazutaka Kondo, Mitsuru Sano, Akio Hiwara, Takehiko Omi, Miho Fujita, Akio Kuwae, Masayasu Iida, Koichi Mogi, and Haruhiko Yokoyama. Conductivity and solvation of li+ ions of LiPF6 in propylene carbonate solutions. *The Journal of Physical Chemistry B*, 104(20):5040–5044, 2000.

[37] T. Fromling, M. Kunze, M. Schonhoff, J. Sundermeyer, and B. Roling. Enhanced lithium trans-

39

ference numbers in ionic liquid electrolytes. *The Journal of Physical Chemistry B*, 112(41):12985–12990, 2008.

[38] C. Capiglia, Y. Saito, H. Kageyama, P. Mustarelli, T. Iwamoto, T. Tabuchi, and H. Tukamoto. Li-7 and f-19 diffusion coefficients and thermal properties of non-aqueous electrolyte solutions for rechargeable lithium batteries. *Journal of Power Sources*, 81Ũ82:859Ũ862, 1999.

[39] K. Hayamizu and W.S. Price. A new type of sample tube for reducing convection effects in PGSE-NMR measurements of self-diffusion coefficients of liquid samples. *Journal of Magnetic Resonance*, 167(2):328–333, 2004.

[40] A.M. Christie and C.A. Vincent. Conductivities of selected lithium salt complexes in propylene carbonate. *The Journal of Physical Chemistry*, 100(11):4618–4621, 1996.

[41] M.S. Ding and T.R. Jow. Conductivity and viscosity of PC-DEC and PC-EC solutions of LiPF6. *Journal of The Electrochemical Society*, 150(5):A620–A628, 2003.

[42] M.S. Ding, K. Xu, and T.R. Jow. Conductivity and viscosity of PC-DEC and PC-EC solutions of LiBOB. *Journal of The Electrochemical Society*, 152(1):A132–A140, 2005.

[43] M.S. Ding. Electrolytic conductivity and glass transition temperatures as functions of salt content, solvent composition, or temperature for LiBF4 in propylene carbonate + diethyl carbonate. *Journal of Chemical & Engineering Data*, 49(4):1102–1109, 2004.

[44] J. Cruickshank, H. V. St. A. Hubbard, N. Boden, and I. M. Ward. The role of ionic salts in determining t-g and ionic-conductivity in concentrated peg electrolyte-solutions. *Polymer*, 36 (19):3779–3781, 1995.

[45] K. Hayamizu, E. Akiba, T. Bando, and Y. Aihara. 1h, 7li, and 19f nuclear magnetic resonance and ionic conductivity studies for liquid electrolytes composed of glymes and polyetheneglycol dimethyl ethers of CH3O(CH2CH2O)nCH3 (n = 3-50) doped with LiN(SO2CF3)2. *The Journal of Chemical Physics*, 117(12):5929–5939, 2002.

[46] T.J. Simons, P.C. Howlett, A.A.J. Torriero, D.R. MacFarlane, and M. Forsyth. Electrochemical, transport, and spectroscopic properties of 1-ethyl-3-methylimidazolium ionic liquid electrolytes containing zinc dicyanamide. *The Journal of Physical Chemistry C*, 117(6):2662–2669, 2013.

[47] Y. Aihara, S. Arai, and K. Hayamizu. Ionic conductivity, dsc and self diffusion coefficients of lithium, anion, polymer, and solvent of polymer gel electrolytes: the structure of the gels and the diffusion mechanism of the ions. *Electrochimica Acta*, 45:1321–1326, 2000.

[48] J.F. Casteel and E.S. Amis. Specific conductance of concentrated solutions of magnesium salts in water-ethanol system. *Journal of Chemical and Engineering Data*, 17(1):55–59, 1972.

[49] A. de Diego, J.M. Madariaga, and E. Chapela. Empirical model of general application to fit (k,c,t) experimental data from concentrated aqueous electrolyte solutions. *Electrochimica Acta*, 42(9):1449–1456, 1997.

[50] M.S. Ding. Casteel-amis equation: Its extension from univariate to multivariate and its use as a two-parameter function. *Journal of Chemical & Engineering Data*, 49(5):1469–1474, 2004.

[51] Q. Zhang, S. Sun, S. Pitula, Q. Liu, U. Welz-Biermann, and J. Zhang. Electrical conductivity of solutions of ionic liquids with methanol, ethanol, acetonitrile, and propylene carbonate. *Journal of*

40

Chemical & Engineering Data, 56(12):4659–4664, 2011.

[52] G. Jones and M. Dole. The viscosity of aqueous solutions of strong electrolytes with special reference to barium chloride. *Journal of the American Chemical Society*, 51:2950, 1929.

[53] J. Jiang and S.I. Sandler. A new model for the viscosity of electrolyte solutions. *Industrial & Engineering Chemistry Research*, 42(25):6267–6272, 2003.

[54] H. Jenkins, B. Donald, and Y. Marcus. Viscosity b-coefficients of ions in solution. *Chemical Reviews*, 95(8):2695–2724, 1995.

[55] G. Jones and S.K. Talley. The viscosity of aqueous solutions as a function of the concentration. *Journal of the American Chemical Society*, 55(2):624–642, 1933.

[56] M. Kaminsky. *Z. Phys. Chem.*, 12:206, 1957.

[57] G. Hefter, P.M. May, P. Sipos, and A. Stanley. Viscosities of concentrated electrolyte solutions. *Journal of Molecular Liquids*, 103-104:261–273, 2003.

[58] A.L. Horvath. *Handbook of aqueous electrolyte solutions: physical properties, estimation and correlation methods.* Ellis Horwood, 1985.

[59] M. Deepa, N. Sharma, S.A. Agnihotry, S. Singh, T. Lal, and R. Chandra. Conductivity and viscosity of liquid and gel electrolytes based on liclo4, lin(cf3so2)(2) and pmma. *Solid State Ionics*, 152Ű153:253Ű 258, 2002.

[60] K. Hayamizu, A. Matsuo, and J. Arai. A divalent lithium salt Li2B12F12 dissolved in propylene carbonate studied by nmr methods. *Journal of The Electrochemical Society*, 156(9):A744–A750, 2009.

[61] M. Takeuchi, Y. Kameda, Y. Umebayashi, S. Ogawa, T. Sonoda, S. Ishiguro, M. Fujita, and M. Sano. Ion-ion interactions of lipf6 and libf4 in propylene carbonate solutions. *Journal of Molecular Liquids*, 148:99–108, 2009.

[62] R. Olender and A. Nitzan. Ion solvation and association in complex solvents: Theoretical considerations. *Electrochimica Acta*, 37(9):1505–1509, 1992.

[63] M. Forsyth, V.A. Payne, M.A. Ratner, S.W. de Leeuw, and D.F. Shriver. Molecular dynamics simulations of highly concentrated salt solutions: Structural and transport effects in polymer electrolytes. *Solid State Ionics*, 53-56, Part 2:1011–1026, 1992.

[64] R. Zarrougui, M. Dhahbi, and D. Lemordant. Effect of temperature and composition on the transport and thermodynamic properties of binary mixtures of ionic liquid n-butyl-n-methylpyrrolidinium bis(trifluoromethanesulfonyl)imide and propylene carbonate. *Journal of Solution Chemistry*, 39(7):921–942, 2010.

[65] K. Umemoto N. Matsuura. Formulation of stokes radii in DMF, DMSO and propylene carbonate with solvent structure cavity size as parameter. *Bulletin of The Chemical Society of Japan - BULL CHEM SOC JPN*, 48(8):2253–2257, 1975.

[66] M. Ue. Mobility and ionic association of lithium and quaternary ammonium salts in propylene carbonate and gamma-Řbutyrolactone. *Journal of The Electrochemical Society*, 141(12):3336–3342, 1994.

[67] Y. Saito, H. Yamamoto, O. Nakamura, H. Kageyama, H. Ishikawa, T. Miyoshi, and M. Matsuoka.

41

Determination of ionic self-diffusion coefficients of lithium electrolytes using the pulsed field gradient nmr. *Journal of Power Sources*, 81-82:772–776, 1999.

[68] O. Soderman, W.S. Price, M. Schonhoff, and D. Topgaard. NMR diffusometry applied to liquids. *Journal of Molecular Liquids*, 156(1):38–44, 2010.

[69] M. Ue. Ionic radius of (cf3so2)3c - and applicability of stokes law to its propylene carbonate solution. *Journal of The Electrochemical Society*, 143(11):L270–L272, 1996.

42